Available online at www.sciencedirect.com
SCIENCE DIRECT®
Journal of Power Sources 140 (2005) 145–150
JOURNAL OF POWER SOURCES
www.elsevier.com/locate/jpowsour

Short communication

Electrochemical characterization of high-performance $LiNi_{0.8}Co_{0.2}O_2$ cathode materials for rechargeable lithium batteries

Si Hyoung Oh, Woon Tae Jeong, Won Il Cho*, Byung Won Cho, Kyoungja Woo

Eco-Nano Research Center, Korea Institute of Science and Technology, P.O. Box 131, Cheongryang, Seoul 136-791, Korea

Received 15 July 2004; received in revised form 20 July 2004; accepted 27 July 2004
Available online 25 September 2004

Abstract

The cathode material, $LiNi_{0.8}Co_{0.2}O_2$ was synthesized by acid dissolution method using lithium carbonate, nickel hydroxide (carbonate), cobalt hydroxide (carbonate) as insoluble starting materials, and acrylic acid, which acts as an organic acid as well as a chelating agent. Structural and chemical characterization of the spray-dried xerogel precursor was performed through its compositional and thermogravimetric analysis (TGA), which shows that the xerogel can be expressed as $Li[MA]_3$, where M is the transition metal atom. The electrochemical performance of the synthesized powder was tested manufacturing the coin-type cells with lithium metal as an anode material. With the voltage range of 3.0–4.2 V, the capacity retentions after 50 cycles were 98.6 and 94.5%, respectively, for the powders calcined at 800 °C for 15 and 20 h. At the rate capability test, discharge capacity ratio between 3.0 and 0.5 C rate is about 91–84% till 60 cycles.

Keywords: $LiNi_{0.8}Co_{0.2}O_2$; Acid dissolution; Hydroxide; Carbonate; Spray drying

1. Introduction

Lithium secondary batteries are currently used as the main rechargeable power sources in modern portable electronic devices such as cellular phones, personal digital assistants (PDAs), laptop computers, camcorders, etc., because of their high output voltage, high specific energy and long life cycle. Lithium cobalt oxide, $LiCoO_2$, is still the only commercialized cathode material due to its excellent electrochemical properties. The high cost and inherent toxicity of this material, however, have led to the intensive investigations on the possible alternatives during the last decade and now $LiNi_{1-x}Co_xO_2$ ($0.2 < x < 0.3$) is considered as one of the most promising candidates because of its less toxicity and higher capacity compared with $LiCoO_2$ [1–4].

Recently, we have developed the acid dissolution process for synthesizing high-performance cathode materials, where the cost-effective starting materials are dissolved by strong organic acid. In this work, we have synthesized $LiNi_{0.8}Co_{0.2}O_2$, a promising alternative of $LiCoO_2$, by acid dissolution method and its electrochemical properties were investigated.

2. Experimental

The acid dissolution method was employed to synthesize the high-performance $LiCo_{0.2}Ni_{0.8}O_2$, which had two different calcination times (CT). Proper amount of acrylic acid (CH_2=CHCOOH) considering acid to metal ion ratio R equal to 4, was weighed and dissolved in distilled water. The stoichiometric amount of insoluble starting materials, Li_2CO_3 (K_{sp} = 2.5 × 10^{-2})[1], $Ni(OH)_2$ (K_{sp} = 5.48 × 10^{-16}), and $Co(OH)_2$ (K_{sp} = 1.6 × 10^{-15}) [5] were also weighed and dissolved in the acid solution into a complete solution under constant stirring at 80 °C. After that, the solution was cooled down and the pH was measured around 4.18 at room

* Corresponding author. Tel.: +82 2 958 5226; fax: +82 2 958 5229.
E-mail address: wonic@kist.re.kr (W.I. Cho).

[1] Solubility product constant, (K_{sp}) = 2.5 × 10^{-2}

0378-7753/$ – see front matter © 2004 Elsevier B.V. All rights reserved.
doi:10.1016/j.jpowsour.2004.07.030

temperature. The solution was then spray-dried to obtain xerogel of the precursor solution. Thermogravimetric analysis (TGA)/differential scanning calorimetry (DSC) was performed in air at a heating rate of 5 °C min^{-1} for the xerogel obtained. After that, the xerogel was collected and subjected to further two-step heat treatment at 500 °C for 6 h in air and, subsequently, at 800 °C for 15 or 20 h in the flowing oxygen atmosphere.

Structural properties of the compounds were studied by the X-ray diffraction technique (XRD). Chemical analysis of the synthesized material was carried out with an atomic absorption spectrophotometer (AAS) and inductively coupled plasma-atomic emission spectrometer (ICP-AES). The elemental analysis was for confirming the stoichiometry of the products. The surface and particle morphology of the synthesized materials were analyzed by SEM images. The electrochemical cycling performance of the materials was studied by assembling coin-type cells (CR2032), and the cells were galvanostatically cycled at a 0.5 C rate (1 C = 140 mA h g^{-1}) between 3.0 and 4.2 or 4.3 V in a multi-channel battery tester. The rate capability of this material was investigated by charging the cell at a 0.5 C rate, while discharging it at a rate of 0.5, 1.0, 2.0, and 3.0 C, in sequence. The synthesized cathode materials were mixed with 8% carbon black and 5% polyvinylidene fluoride (PVdF) as a binder, and made into a slurry using *N*-methylpyrrolidinone (NMP) as a solvent and coated onto aluminum foil which was used as a current collector. The typical loading rate of active materials was about 7.5 mg cm^{-2} with 120 μm thickness. The coated aluminum foil was allowed to dry overnight at room temperature and then it was roller pressed to better adhere the materials to the current collector. The cathodes were punched from the foil. The cells were assembled inside drying room using lithium metal as an anode, polypropylene (PP) film as a separator and a 1 M $LiPF_6$ in 1:1:1 (ethylene carbonate (EC)–ethylmethyl carbonate (EMC)–dimethyl carbonate (DMC)) co-solvent as an electrolyte.

3. Results and discussions

The acid dissolution process utilizes the dissolution of the starting materials such as metal carbonates and metal hydroxides, which are insoluble in normal aqueous solution. But these materials are forced to dissolve by an organic acid, which also acts as a chelating agent. As an insoluble lithium source, lithium carbonate in acidic solution dissolves into aqueous ions, releasing CO_2 gas.

$$\tfrac{1}{2}Li_2CO_3 + HA \rightarrow Li^+ + \tfrac{1}{2}CO_2 \uparrow + \tfrac{1}{2}H_2O + A^- \quad (1)$$

where HA is the organic acid used and A^- is the anion of the organic acid. Transition metal hydroxides ($M(OH)_2$, where M denotes nickel or cobalt) are among the insoluble metal sources. They also dissolve in acidic solution but combines with chelating agents to be complex ions.

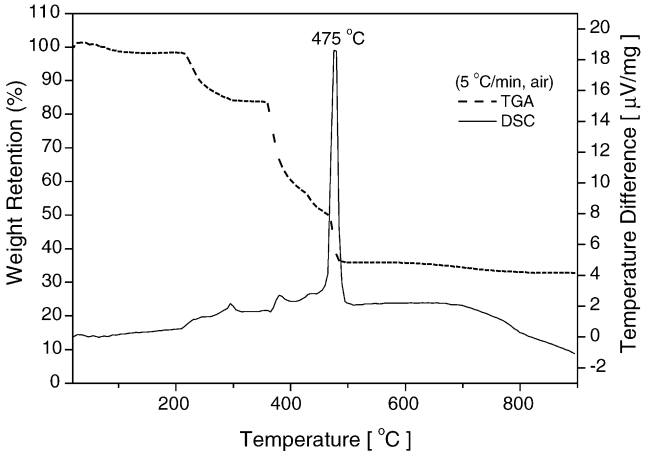

Fig. 1. TGA/DSC curves of spray-dried xerogel, $Li[MA_3]$.

$$M(OH)_2 + 2HA \rightarrow M^{2+} + 2H_2O + 2A^- \quad (2)$$

$$M^{2+} + 3A^- \rightarrow [MA_3]^- \quad (3)$$

As the solvent is eliminated by spray drying process, the solution transforms into a micro-size xerogel powder.

$$\tfrac{1}{2}Li_2CO_3 + M(OH)_2 + 3HA \rightarrow Li^+ + [MA_3]^- + \tfrac{1}{2}CO_2 \uparrow + \tfrac{5}{2}H_2O \xrightarrow{\text{solvent evaporation}} Li[MA_3] \quad (4)$$

In case metal carbonates (MCO_3) are to be used as an insoluble metal source or lithium hydroxide (LiOH) is used instead of lithium carbonate, similar reactions occur and final xerogel powder will be the same chemistry. From Eq. (4), it is clear that after solvent evaporation, the xerogel has a molecularly homogeneous atomic arrangement and there exists no other redundant ionic group such as acetates, nitrates within the xerogel occurring when metal nitrates or metal acetates are used as starting materials, which, we believe, has a detrimental effect on the final product, and which is why we used metal hydroxides or carbonates as starting materials. From Eq. (4), the theoretical acid to metal ion ratio R[2] of the process can be deduced to 1.5. But in the actual experiment, the acid was intentionally inserted in excess in order to facilitate the quick and complete dissolution of the insoluble source materials. When lithium carbonate, cobalt(II) hydroxide, nickel(II) hydroxide and acrylic acid are used, appropriate *R*-value was found to be 4, but the solution needed heating up to 80 °C for the complete dissolution of hydroxide species.

Fig. 1 shows the TGA/DSC curves of the spray-dried xerogel, $Li[MA_3]$. The TGA curve shows that minor weight losses occur in the temperature around 100 °C and two steps of major weight losses of 65% around 250 °C and between

[2] R = Σ number of proton/Σ number of metal ion

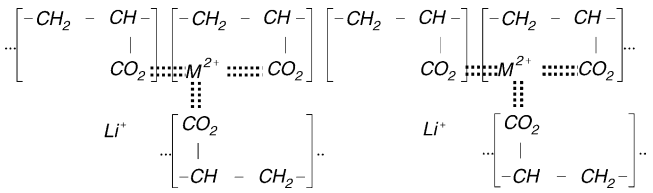

Fig. 2. Supposed structure of spray-dried xerogel, Li[MA_3].

350 and 500 °C corresponding to the one sharp exothermic peak in the DSC curve around 475 °C. There was no apparent weight change after 500 °C. From Eq. (4), when acrylic acid is used for chelating agent, the weight ratio of $LiNi_{0.8}Co_{0.2}O_2$ to Li[MA_3] is about 0.35, which is dependent on the specific acid used. Considering excess acrylic acid is used to facilitate the dissolution of starting materials, TGA results show the validity of the above analysis. The initial and second weight losses can be attributed to the loss of small amount of water and the burning of the excess acrylic acid present in the xerogel, respectively. Most of the combustion process is initiated in this temperature range 350–500 °C, as evidenced by the larger DSC peak in Fig. 1, which, we believe, is related with the decomposition of Li[MA_3]. The composition analysis of xerogel indicates that the atomic ratio, carbon to transition metal, C/M is near 12 as can be estimated from Table 2(c). This implies that the actual composition of the xerogel is close to Li[MA_3]·HA. Considering that R was equal to 4 in the experiment, where C/M could be calculated as 24, it can be said that there is loss or evaporation of excess acrylic acid, which did not form chelates with transition metal, during spray drying process. In Fig. 2, it was shown that the supposed structure of Li[MA_3] xerogel are the polymerization of the cobalt complex unit, where three acrylic acid anions are combined with a single Co^{2+} ion, to be a chelate ion with which single Li ion is ionically combined.

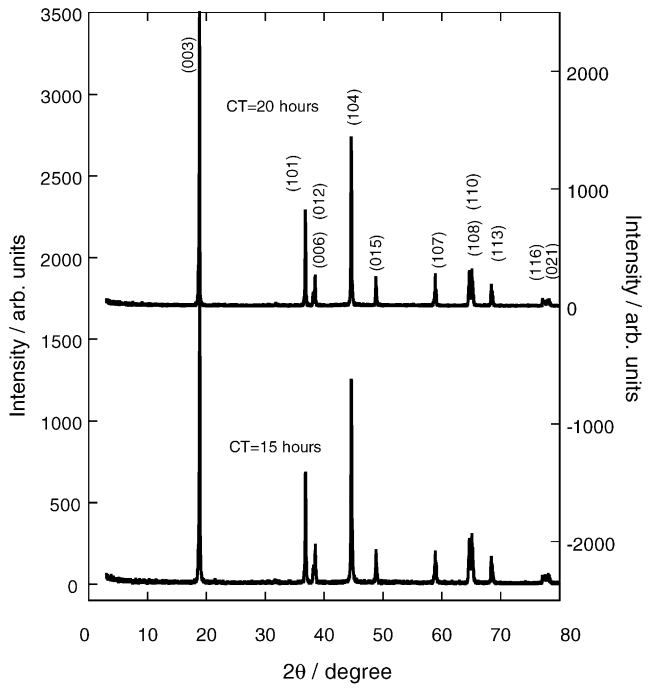

Fig. 3. XRD patterns for the powders synthesized at 800 °C for 15 h and 20 h.

Table 1
Lattice parameters, unit cell volume and structural parameters for $LiNi_{0.8}Co_{0.2}O_2$ synthesized at 800 °C for (a) 15 and (b) 20 h in the oxygen atmosphere

	a (Å)	c (Å)	c/a	I_{003}/I_{104}	Cell volume (Å^3)
(a)	2.875	14.221	4.946	1.471	101.82
(b)	2.868	14.185	4.946	1.409	101.03

The typical X-ray diffraction spectra for the compounds calcined at 800 °C in the oxygen atmosphere are given in Fig. 3. Both the XRD patterns reveal the formation of a phase indexable to the layered α-$NaFeO_2$ structure assuming a hexagonal setting in the $R\bar{3}m$ space group. The diffraction patterns show clear splittings of the hexagonal characteristic doublets (0 0 6)/(1 0 2) and (1 0 8)/(1 1 0), which is a distinct indication of good hexagonal ordering. The lattice parameters were calculated by least square method using 10 diffraction

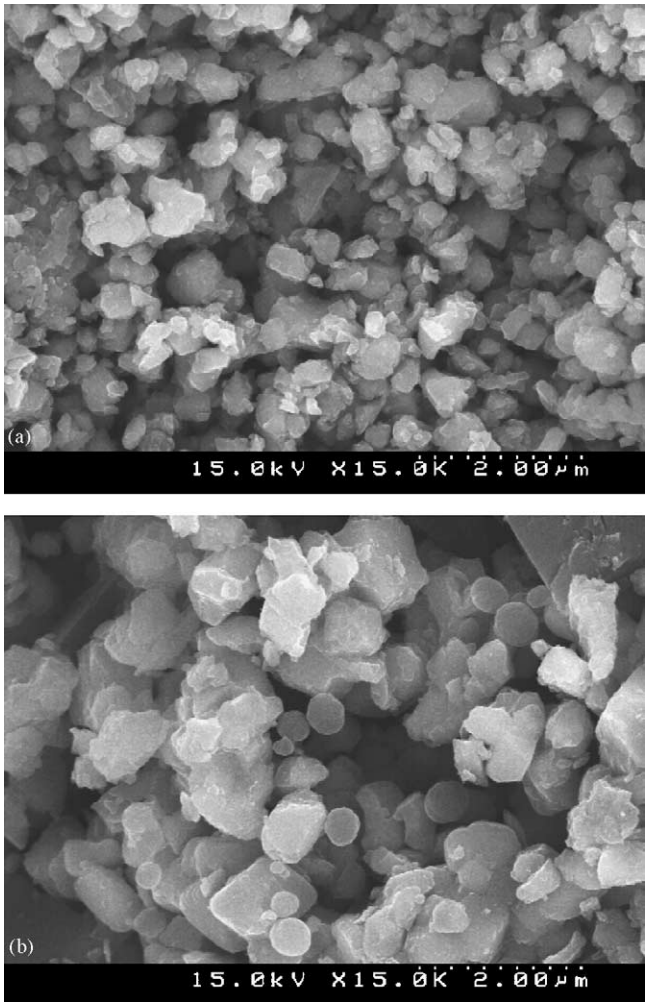

Fig. 4. SEM images of powders synthesized at 800 °C for (a) 15 h and (b) 20 h.

Table 2
Composition analysis for $LiNi_{0.8}Co_{0.2}O_2$ synthesized at 800 °C for (a) 15 h and (b) 20 h in the oxygen atmosphere, and (c) for $Li[MA_3]$ xerogel precursor

Composition	Li	Ni	Co	Li/(Co + Ni)
(a)	1.034	0.753	0.202	1.083
(b)	1.026	0.762	0.204	1.063
Composition	Li	Ni	Co	C
(c)	0.280	0.210	0.053	3.239

lines and the results together with the other structural parameters are tabulated in Table 1. The lattice parameters of powders calcined for 15 h were slightly smaller than those for 20 h, although the ratio, *c*/*a*, remained unchanged during extended calcination time. The intensity ratio of (0 0 3) and (1 0 4) peaks (I_{003}/I_{104}) has been considered as the degree of cation mixing by many researchers [6,7], and reversible capacity is known to decrease when the ratio is less than 1.2 [8–10]. In this work, the ratios were found to be 1.471 and 1.409, which is greater than the critical value.

The SEM images of $LiNi_{0.8}Co_{0.2}O_2$ polycrystalline powders calcined at 800 °C for 15 and 20 h are shown in Fig. 4. Both the images show the homogeneous distribution and similar shapes of the particles with submicron size, but the powders calcined for 15 h are smaller in size than those for 20 h. The actual compositions of the synthesized powders were analyzed by the atomic absorption spectrophotometer (AAS) and inductively coupled plasma-atomic emission spectrometer (ICP-AES). As can be seen from Table 2(a) and (b), the results of the elemental analysis show that the nickel content is slightly lower than the targeted one, which we think, results from the loss during synthesis process. But, the ratio of lithium to transition metal is almost stoichiometric value, 1.

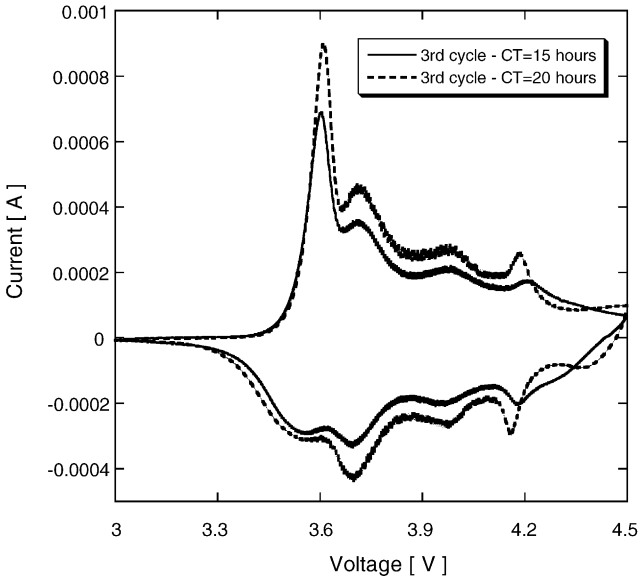

Fig. 5. Cyclic voltammogram (3rd cycles) of the half-cell, $LiNi_{0.8}Co_{0.2}O_2$/$LiPF_6$/Li with voltage range of 3.0–4.5 V at a scan rate of 0.02 mV s^{-1}, for the powders synthesized at 800 °C for 15 and 20 h.

Cyclic voltammogram (3rd cycle) of the powders synthesized at 800 °C for 15 and 20 h at a scan rate of 0.02 mV s^{-1} between 3.0 and 4.5 V are shown in Fig. 5. They show the typical cyclic curves of similar shape, found in other literatures [11–13]. The discharge capacities and corresponding discharge profiles of the half-cell, $LiNi_{0.8}Co_{0.2}O_2$/$LiPF_6$ in (EC + EMC + DMC)/Li, with respect to the cycling with the cut-off voltage 4.2 or 4.3 V at 0.5 °C rate are given in Fig. 6(a) and Fig. 7. For the compound synthesized at 800 °C for 15 h, the discharge capacities at first cycle were 142.3 and 149.8 mA h g^{-1}, while capacity retentions after 50 cycles were 98.6 and 95.1% for cut-off voltage 4.2 and 4.3 V,

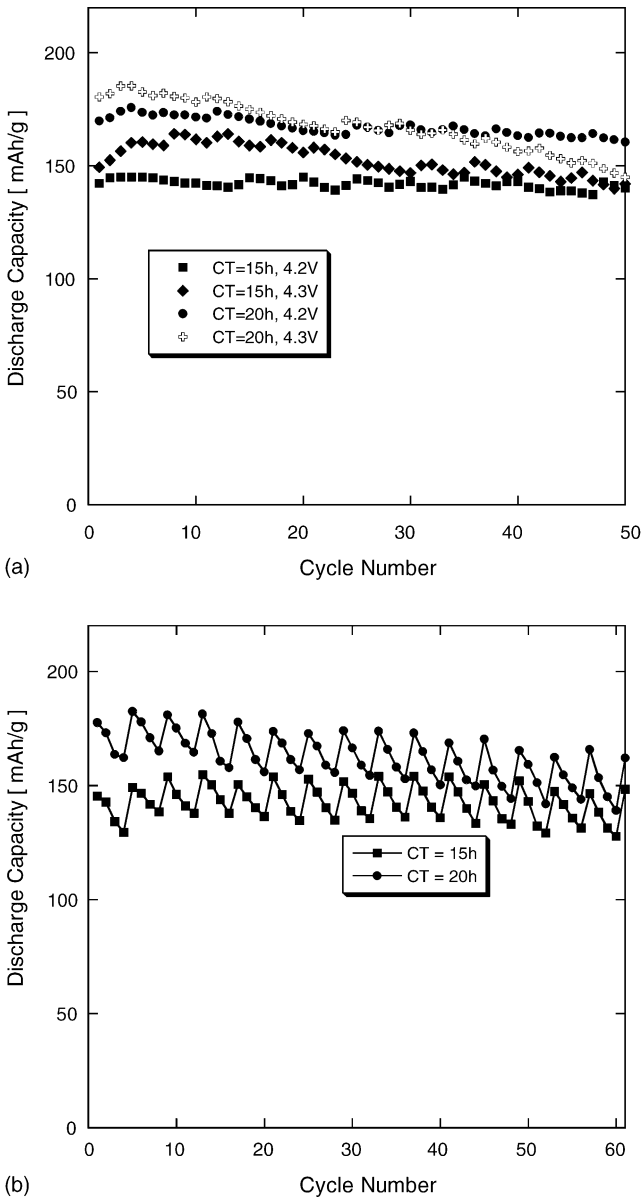

Fig. 6. (a) Cyclic discharge capacities of the half-cell, $LiNi_{0.8}Co_{0.2}O_2$/$LiPF_6$/Li with voltage range of 3.0–4.2 and 4.3 V, at 0.5 C rate, for the powders synthesized at 800 °C for 15 and 20 h, and (b) rate capability cycled between 3.0 and 4.2 V, charging at 0.5 C rate, while discharging at 0.5, 1.0, 2.0, and 3.0 C in sequence.

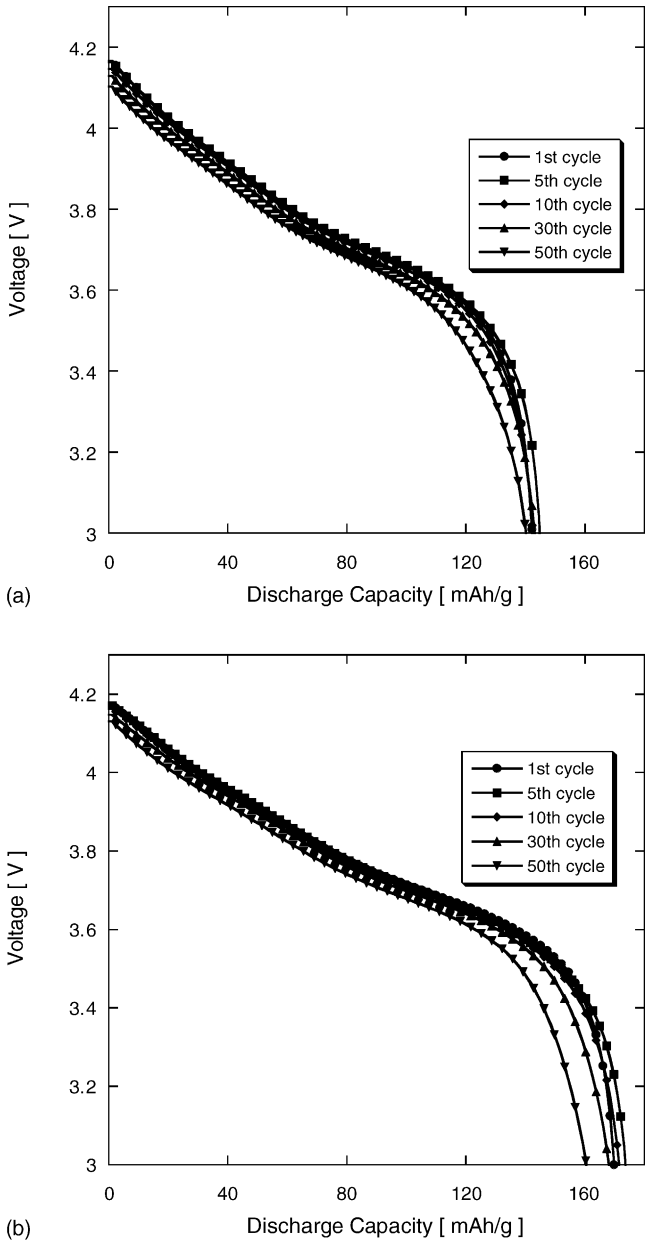

Fig. 7. Discharge profiles of the half-cell, $LiNi_{0.8}Co_{0.2}O_2$/$LiPF_6$/Li with voltage range of 3.0–4.2 V, at 0.5 C rate, for the powders synthesized at 800 °C for (a) 15 and (b) 20 h.

respectively. For the compound synthesized at 800 °C for 20 h, the discharge capacities at first cycle was 169.8 and 180.5 mA h g^{-1}, while the capacity retentions after 50 cycles were 94.5 and 80.2% for the cut-off voltage of 4.2 and 4.3 V, respectively. In both cases, the profiles of discharge curves showed a good retention of original shape even after 50 cycles when cut-off voltage was 4.2 V as shown in Fig. 7(a) and (b). Accordingly, the initial discharge capacity is greater when the calcination time is 20 h, which implies that calcination time of 15 h is not long enough, but for capacity retention, calcination time of 15 h showed better cyclic performance.

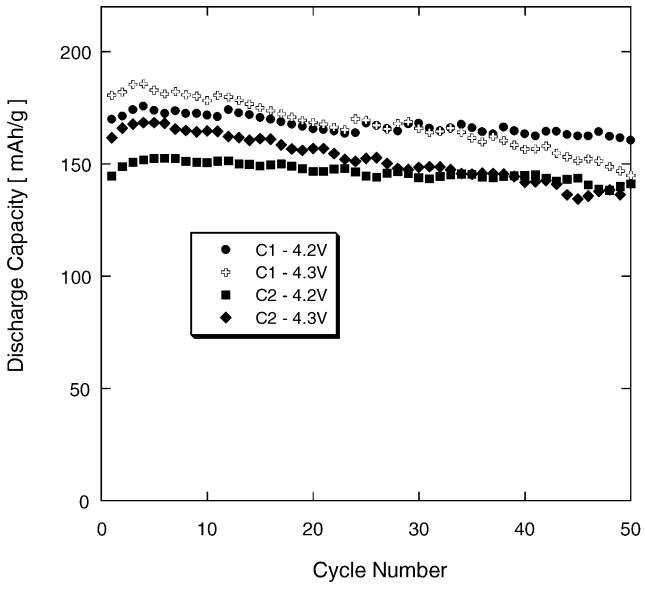

Fig. 8. Comparison of cyclic performance of the half-cell, $LiNi_{0.8}Co_{0.2}O_2$/$LiPF_6$/Li with voltage range of 3.0–4.2 and 4.3 V, at 0.5 C rate, for the powders synthesized by different starting materials set—C1: Li_2CO_3 + $Ni(OH)_2$ + $Co(OH)_2$, calcined at 800 °C for 20 h; C2: Li_2CO_3 + $NiCO_3{\cdot}2Ni(OH)_2{\cdot}H_2O$ + $CoCO_3$, calcined at 800 °C for 20 h.

Fig. 6(b) shows that the rate capability of the synthesized powders by discharging the cell at four different C-rates (0.5, 1.0, 2.0, and 3.0 C), while charging it at 0.5 C rate, successively between 3.0 and 4.2 V. It shows the ratios of discharge capacities between 4th (3 C rate) and 1st (0.5 C rate) cycle are 89 and 91%, while 60th (3 C rate)/57th (0.5 C rate) are 87 and 84% for calcination time of 15 and 20 h, respectively. Thus, both the materials showed similar and good rate capability. The effect of different starting materials on the cyclic performance was compared by synthesizing $LiNi_{0.8}Co_{0.2}O_2$ using carbonate species, $CoCO_3$ and $NiCO_3{\cdot}2Ni(OH)_2{\cdot}H_2O$ instead of $Co(OH)_2$ and $Ni(OH)_2$ and the results are shown in Fig. 8. The similar cyclic behavior is expected, because, as mentioned earlier, the same precursor xerogel, $Li[MA]_3$, is produced, regardless of two different starting materials set, since the carbonate of the metal compound reacts with acid to produce CO_2 gas. The capacity retentions with cycling of the two specimens are very similar, although the initial capacities of the C1 are smaller.

4. Conclusion

The cathode material, $LiNi_{0.8}Co_{0.2}O_2$, was synthesized by acid dissolution method using lithium carbonate, nickel hydroxide (carbonate), cobalt hydroxide (carbonate) as insoluble starting materials, and acrylic acid, which acts as an organic acid as well as a chelating agent. Structural and chemical characterization of the spray-dried xerogel pre-

cursor was performed through its compositional and thermogravimetric analysis, which shows that xerogel can be expressed as $Li[MA]_3$. At the electrochemical measurements, the capacity retentions and rate capabilities of the synthesized powders with cycling were very good. With the cut-off voltage of 4.2 V, the capacity retention after 50 cycles was 98.6 and 94.5%, respectively, for the powders calcined at 800 °C for 15 and 20 h. At the rate capability test, discharge capacity ratio between 3.0 and 0.5 C rate is about 91–84% till 60 cycles. Thus, we think that $LiNi_{0.8}Co_{0.2}O_2$ cathode materials synthesized by the acid dissolution method can be one of the promising alternatives of $LiCoO_2$.

Acknowledgement

This research was supported by a grant (code no. 04K1501-01910) from 'Center for Nanostructured Materials Technology' under '21st Century Frontier R&D Programs' of the Ministry of Science and Technology, Korea

References

[1] W. Li, J.C. Currie, J. Electrochem. Soc. 144 (1997) 2773.
[2] J. Cho, G.B. Kim, H.S. Lim, J. Electrochem. Soc. 146 (1999) 3571.
[3] J. Cho, H.S. Jung, Y.C. Park, G.B. Kim, H.S. Lim, J. Electrochem. Soc. 147 (2000) 15.
[4] J. Cho, Chem. Mater. 12 (2000) 3089.
[5] R. Lide David, Handbook of Chemistry and Physics, 83rd ed., 2002.
[6] Y.M. Choi, S.I. Pyun, S.I. Moon, Y.E. Hyung, J. Power Sources 72 (1998) 83.
[7] T. Ohzuku, A. Ueda, M. Nagayama, J. Electrochem. Soc. 140 (1993) 1862.
[8] G.X. Wang, S. Zhong, D.H. Bradhurst, S.X. Dou, H.K. Liu, J. Power Sources 76 (1998) 141.
[9] T. Ohzuku, A. Ueda, M. Nagayama, Y. Iwakoshi, H. Komori, Electrochim. Acta 38 (1993) 1159.
[10] D. Aurbach, K. Gamolsky, B. Markovsky, G. Salitra, Y. Gofer, U. Heider, R. Oesten, M. Schmidt, J. Electrochem. Soc. 147 (2000) 1332.
[11] E. Levi, M.D. Levi, G. Salitra, D. Aurbach, R. Oesten, U. Heider, L. Heider, Solid State Ionics 126 (1999) 97.
[12] C.J. Han, J.H. Yoon, W.I. Cho, H. Jang, J. Power Sources 136 (2004) 132.
[13] S.C. Park, Y.S. Han, P.S. Lee, S. Ahn, H.M. Lee, J.Y. Lee, J. Power Sources 102 (2001) 130.